

Growth and Development of GaInAsP for Use in High-Efficiency Solar Cells

Final Subcontract Report
1 July 1991 – 30 December 1993

P. R. Sharps
Research Triangle Institute
Research Triangle Park, North Carolina

NREL technical monitor: J. Benner



National Renewable Energy Laboratory
1617 Cole Boulevard
Golden, Colorado 80401-3393

A national laboratory of the U.S. Department of Energy
Managed by Midwest Research Institute
for the U.S. Department of Energy
under contract No. DE-AC36-83CH10093

MASTER

Prepared under Subcontract No. XM-0-19142-3

October 1994

DISTRIBUTION OF THIS DOCUMENT IS UNLIMITED

rb

NOTICE

This report was prepared as an account of work sponsored by an agency of the United States government. Neither the United States government nor any agency thereof, nor any of their employees, makes any warranty, express or implied, or assumes any legal liability or responsibility for the accuracy, completeness, or usefulness of any information, apparatus, product, or process disclosed, or represents that its use would not infringe privately owned rights. Reference herein to any specific commercial product, process, or service by trade name, trademark, manufacturer, or otherwise does not necessarily constitute or imply its endorsement, recommendation, or favoring by the United States government or any agency thereof. The views and opinions of authors expressed herein do not necessarily state or reflect those of the United States government or any agency thereof.

Available to DOE and DOE contractors from:
Office of Scientific and Technical Information (OSTI)
P.O. Box 62
Oak Ridge, TN 37831
Prices available by calling (615) 576-8401

Available to the public from:
National Technical Information Service (NTIS)
U.S. Department of Commerce
5285 Port Royal Road
Springfield, VA 22161
(703) 487-4650



DISCLAIMER

Portions of this document may be illegible electronic image products. Images are produced from the best available original document.

Table of Contents

1.0 Introduction and Summary of Accomplishments	1
1.1 Introduction.....	1
1.2 Summary of Phase I and Phase II Accomplishments.....	1
1.3 Summary of Phase III Accomplishments	2
2.0 Technical Effort.....	3
2.1 Introduction.....	3
2.2 Growth of GaInAsP on Ge.....	3
2.3 GaInAsP Tunnel Diodes	4
2.4 Development of the Ge Cell	8
2.5 Development of the Cascade Structure	13
2.5.1 Cascade Cells Grown on Active Ge Junctions	13
2.5.2 Cascade Cells Grown with Diffused Ge Junctions	19
3.0 Summary and Closing Comments	25
4.0 References	26
5.0 Appendix	27

List of Figures

Fig. 1	Schematic of the GaInAsP tunnel junction grown on Ge.....	6
Fig. 2	Current-voltage curve for the GaInAsP tunnel diode shown in Fig.1.....	6
Fig. 3	Schematic of the GaInAsP/GaAs heterotunnel junction grown on Ge.....	7
Fig. 4	Schematic of the n-on-p Ge cell.....	9
Fig. 5	Current-voltage curve for the n-on-p Ge cell.....	10
Fig. 6	Schematic of the p-on-n Ge cell.....	11
Fig. 7	Current-voltage curve for the p-on-n Ge cell.....	12
Fig. 8	Schematic of the cascade cell that was grown on the p-on-n Ge junction.....	14
Fig. 9	Typical current-voltage curve for the type of cell shown in Fig. 8.....	15
Fig. 10	Schematic of the cascade cell that was grown on the n-on-p Ge junction.....	17
Fig. 11	Current-voltage curve for the structure shown in Fig. 10.....	18
Fig. 12	Current-voltage curve of a second type for the structure shown in Fig. 10.....	18
Fig. 13	Schematic of the cascade cell that was grown on the n-type Ge substrate.....	20
Fig. 14	Current-voltage curve for the structure shown in Fig. 13.....	21
Fig. 15	Current-voltage curve of a second type for the structure shown in Fig. 13.....	21
Fig. 16	Schematic of the cascade cell that was grown on the p-type Ge substrate.....	23
Fig. 17	Current-voltage for the structure shown in Fig. 16.....	24

1.0 Introduction and Summary of Accomplishments

1.1 Introduction

The purpose of this report is to review the progress that has been made toward achieving the goals of Subcontract No. XM-0-19142-3. The report will focus on the work that has been accomplished during Phase III between July 1, 1992 and November 30, 1993. The overall goals of the program are:

1. to develop the necessary technology to grow high-efficiency GaInAsP layers that are lattice-matched to GaAs and Ge,
2. to demonstrate high-efficiency GaInAsP single junction solar cells, and
3. to demonstrate GaInAsP/Ge cascade solar cells suitable for operation under concentrated (500x) sunlight.

1.2 Summary of Phase I and Phase II Accomplishments

The major accomplishments of Phase I include:

1. modification of the organometallic vapor phase epitaxy (OMVPE) reactor for growth of GaInAsP,
2. growth of $\text{Ga}_{0.84}\text{In}_{0.16}\text{As}_{0.68}\text{P}_{0.32}$ (hereafter referred to as GaInAsP) lattice-matched to GaAs having a band gap of 1.55 eV, and growth of the same composition on Ge,
3. demonstration of the compositional uniformity of the GaInAsP films,
4. control and calibration of the n- and p-type doping in the films,
5. growth of the double-heterostructure for both the n-type material and the p-type material, and measurement of minority carrier lifetimes of 37 ns and 3.7 ns in the respective materials,
6. demonstration of a p-on-n solar cell with an active area efficiency of 18.8% under AM1.5 illumination, and
7. growth of higher band gap compositions of GaInAsP.

The major accomplishments of Phase II include:

1. fabrication of p-on-n and n-on-p GaInAsP cells on GaAs, with the n-on-p cell demonstrating a 1-sun (AM 1.5D) active area efficiency of 21.8% and a 10-sun (AM 1.5) active area efficiency of 23.4%, as measured at NREL,
2. evaluation of $\text{Al}_x\text{Ga}_{(1-x)}\text{As}$, GaInP_2 , and AlInP_2 window layers, and
3. fabrication of GaInAsP cells on Ge, with the demonstration of a p-on-n GaInAsP cell grown on Ge with a 1-sun (AM1.5) active area efficiency of 14.4%.

The Annual Reports for 1991 and 1992 contain further discussion regarding the above accomplishments.

1.3 Summary of Phase III Accomplishments

Progress has continued during Phase III of the contract. The major accomplishments include:

1. demonstration of a GaInAsP tunnel diode for use as an interconnect in the GaInAsP/Ge cascade cell, and
2. demonstration of a GaInAsP/Ge cascade cell.

The development of the GaInAsP tunnel diode is a major accomplishment because it allows for the GaInAsP and Ge cells to be connected without optical losses for the bottom Ge cell, as say a Ge tunnel diode would cause. The GaInAsP/Ge cascade cell development is significant because of the demonstration of a cascade cell with a new materials system. Further progress made during Phase III is contained in the following pages.

2.0 Technical Effort

2.1 Introduction

The focus of the technical effort for Phase III has been on the following:

1. development of a tunnel diode suitable for use in the GaInAsP/Ge monolithic cascade structure,
2. development of a Ge bottom cell, and
3. development of the final cascade cell structure.

2.2 Growth of GaInAsP on Ge

One technical aspect of the program that has required considerable attention has been the growth of GaInAsP on Ge. The difficulties have involved two issues, nucleation of the GaInAsP on the Ge, and also lattice-matching between the GaInAsP and the Ge.

In regards to nucleation of GaInAsP on Ge, the challenge involves growth of a polar material on a non-polar substrate. Under appropriate conditions, GaAs can be readily nucleated on Ge, and high quality GaAs films grown [1]. In our own work we have found that we can nucleate GaInAsP directly on Ge at the normal GaInAsP growth temperature (675 °C) provided that the H₂ carrier gas flow is increased from 3 liters/min to 8 liters/min and also that the Ge substrates are misoriented by 10° from (100). Without the increase in carrier flow, the GaInAsP films are hazy; with the increase in carrier flow, the films are specular to the eye. It is believed that the increase in carrier flow decreases the growth rate, allowing more time for adatoms to move about the surface and rearrange before being buried by ensuing layers. Varying the growth temperature and trying to nucleate thin layers of GaAs did not lead to specular films. The misorientation of the Ge is also critical. At misorientations of less than 10° from (100) the films are hazy to the eye. The 10° misorientation is necessary to suppress the

formation of anti-phase boundaries (APBs), which commonly occur when polar materials are grown on non-polar materials.

The second difficulty, that of lattice-matching between the GaInAsP and the Ge, is more challenging. The difference in mechanical properties between GaAs and Ge required much more precision lattice-matching when growing on Ge substrates as compared to growing on GaAs substrates. When growing on GaInAsP on GaAs, the epitaxial layer may not be precisely lattice-matched with the substrate, and no apparent bowing of the substrate is seen. However, in growing the same GaInAsP composition on Ge, the slight mismatches between the GaInAsP film and the Ge substrate can cause the substrate to be bowed. A 5 μm GaInAsP film is capable of causing visible bowing in a 350 μm Ge substrate. The thicker the epitaxial film is, the more precise the lattice-matching has to be. With care, GaInAsP films can be grown on Ge substrates with no visible deformation in the substrates. It should be emphasized that great care must be taken to achieve the lattice-matching. In one set of experiments, the composition of the GaInAsP films was varied by about 1% between two runs. In the first run, the Ge substrate and GaInAsP film were bowed one way (up), while in the next run the film and substrate were bowed in the other direction (down). The cause of the deformation in the Ge substrates as compared to the GaAs substrates is due to the difference in the elastic constants of the materials as compared to differences in the thermal expansion coefficients, since the thermal expansion coefficients of Ge and GaAs are virtually identical. As mentioned previously, with considerable care films can be grown that do not distort the Ge substrates.

2.3 GaInAsP Tunnel Diodes

Development of a monolithic cascade cell requires the development of an appropriate interconnect between the component cells. For the GaInAsP/Ge cascade cell, we have

considered four possible tunnel junction interconnects. The first two tunnel diodes were grown as stand-alone devices to test their suitability for cascade use, while the second two tunnel diodes that were examined were only considered within complete cascade structures. Of the first two tunnel diodes, one is an all GaInAsP tunnel junction, while the second is a GaInAsP/GaAs heterotunnel junction. The all GaInAsP tunnel junction has the advantage of not causing any optical losses for light that has passed through the top cell, but has not yet reached the bottom cell. The GaInAsP/GaAs tunnel junction allows for the possibility of nucleating GaAs on Ge, which might improve the material quality of the subsequently grown GaInAsP layers. However, as mentioned previously, our work on the growth of GaInAsP directly on Ge indicated that nucleation of GaInAsP directly on Ge was not a problem, whereas GaAs on Ge was. In any case, both types of tunnel junctions were fabricated to see which one gave a superior performance.

Fig. 1 shows the structure of a p^{++} -on- n^{++} GaInAsP tunnel diode that was grown on Ge. Since there are no optical losses due to the tunnel diode, there are no constraints on the thickness of the layers, i.e., no need to thin the layers to reduce optical losses. Fig. 2 shows the current-voltage curve for the device. Notice in particular the existence of a "kink" in the negative resistance region. This is believed to be due to tunneling occurring between the degenerate bands and a deep level within the band gap, leading to the small increase in the current with increasing voltage in part of the negative resistance region. The peak current is 4.33×10^3 mA/cm², and occurs at a voltage of 65 mV. For a GaInAsP/Ge cascade cell under 10 sun concentration (a current density of approximately 300 mA/cm²), the voltage drop across the tunnel junction is about 4.5 mV, while for 100 sun concentration, the voltage drop is about 45 mV across the tunnel diode. Clearly the tunnel diode is sufficient for 10 sun operation, but for higher concentrations more work needs to be done to improve the tunnel junction interconnect. One possibility lies in pulsed growth of the tunnel diode, which is reported to give tunnel junctions capable of carrying larger currents with lower resistive losses [2].

Metal		
p++-GaInAsP	$\sim 10^{20} \text{ cm}^{-3}$	0.8 μm
n++-GaInAsP	$\sim 10^{20} \text{ cm}^{-3}$	0.8 μm
n-Ge substrate		$\sim 300 \mu\text{m}$
Metal		

Fig. 1 Schematic of the GaInAsP tunnel junction grown on Ge.

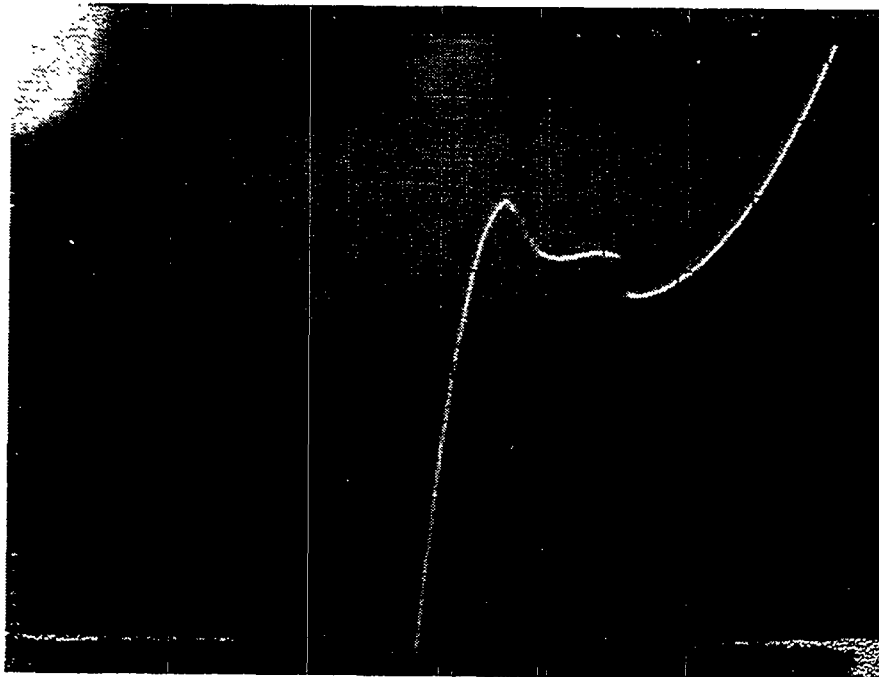


Fig. 2 Current-voltage curve for the GaInAsP tunnel diode shown in Fig. 1. The x-axis scale is 0.1 volts per large division, and the y-axis scale is 2 mA per large division. The area of the tunnel diode is $9 \times 10^{-4} \text{ cm}^2$.

Fig. 3 shows the schematic of the GaInAsP/GaAs heterotunnel junction. The GaAs layer was kept thin to keep optical losses to a minimum. The current-voltage curves for the devices did not show the negative resistance region; rather, poor quality diodes are typically seen, with turn-on voltages of about 0.2 volts and breakdown voltages about the same. We believe that Ge is diffusing through the thin GaAs layer into the p⁺⁺-GaInAsP layer, compensating for the doping, and creating a poor quality junction in the GaInAsP. The GaAs layer has to be kept thin to prevent optical losses, so increasing the thickness of the GaAs layer is not a viable option. The morphology of the films was also not very good. Clearly, a comparison of the first two tunnel diodes indicates that the GaInAsP tunnel junction is the obvious choice. The second two tunnel junctions were both GaInAsP/Ge type heterotunnel diodes, and since they were only grown within complete cascade structures, their discussion will be reserved for Section 2.5, Development of the Cascade Structure.

Metal		
p ⁺⁺ -GaInAsP	~10 ²⁰ cm ⁻³	0.8 μm
n ⁺⁺ -GaAs	~10 ²⁰ cm ⁻³	~500 Å
n-Ge substrate		~300 μm
Metal		

Fig. 3 Schematic of the GaInAsP/GaAs heterotunnel junction grown on Ge.

2.4 Development of the Ge Cell

A number of different configurations were considered for the bottom Ge cell, both as-grown junctions and junctions created by diffusion during growth of the GaInAsP epitaxial layers. The different Ge cell options were considered in order to increase the possible structures that could be considered for the final cascade structure. Initially, both n-on-p and p-on-n Ge cells were grown in a vapor phase epitaxy (VPE) reactor.

Fig. 4 shows a schematic of the n-on-p Ge cell, and Fig. 5 shows the current-voltage curve for the same cell under AM 1.5D illumination. The V_{OC} for the cell is 0.175 volts, the I_{SC} is 2.92 mA, and the fill factor is 0.60. With an active area of 0.141 cm^2 , the active area efficiency of the device is 2.2%. Fig. 6 shows the schematic of the p-on-n Ge cell, and Fig. 7 shows the current-voltage curve for the cell under AM 1.5D illumination. The V_{OC} for the cell is 0.149 volts, the I_{SC} is 3.86 mA, and the fill factor is 0.60. With an active area of 0.141 cm^2 , the active area efficiency of the device is 2.4%.

Based on the results for the Ge cells themselves, there is no clear preference as to cascade cell polarity. Either type of Ge device could be used in a cascade cell. If either of the as-grown Ge devices were incorporated into the cascade structure, they should add approximately 1.2% to the efficiency of the device, i.e., the voltage of the devices would be about the same, while the current would be approximately halved. This is based on the assumption that an appropriate tunnel junction and top cell can be grown on the Ge device without having a deleterious effect on the Ge device.

Metal		
n ⁺⁺ -Ge	~mid 10 ¹⁹ cm ⁻³	0.1 μm
n ⁺ -Ge	~10 ¹⁸ cm ⁻³	1 μm
p-Ge	~10 ¹⁷ cm ⁻³	6 μm
p ⁺ -Ge	~10 ¹⁸ cm ⁻³	0.1 μm
p-Ge substrate		~300 μm
Metal		

Fig. 4 Schematic of the n-on-p Ge cell.

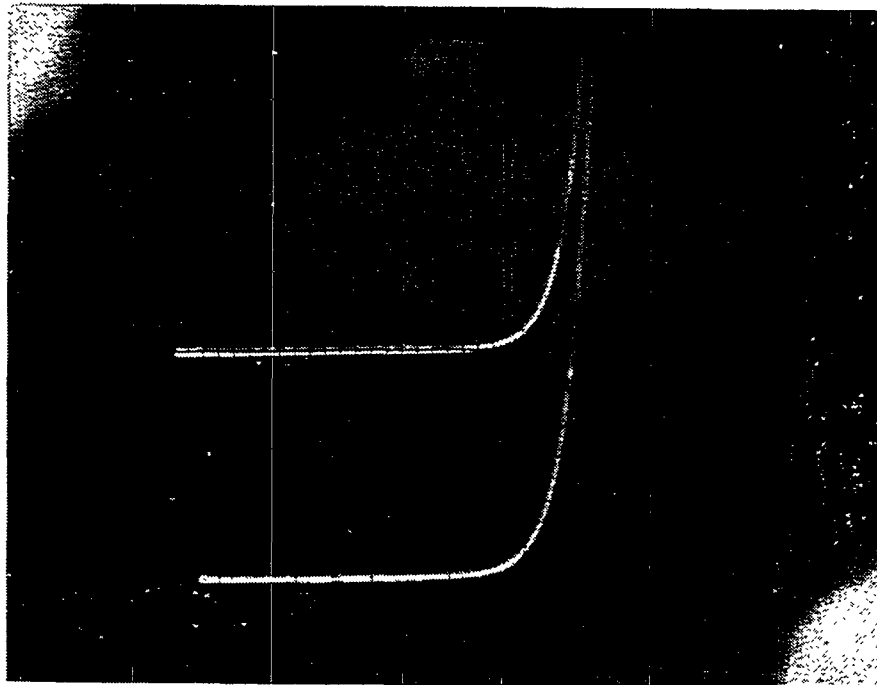


Fig. 5 Current-voltage curve for the n-on-p Ge device, a schematic of which is shown in Fig. 4. The x-axis scale is 0.1 volts/large division, and the y-axis scale is 1 mA/large division.

Metal		
p ⁺⁺ -Ge	~mid 10 ¹⁹ cm ⁻³	0.1 μm
p ⁺ -Ge	~10 ¹⁸ cm ⁻³	1 μm
n-Ge	~10 ¹⁷ cm ⁻³	6 μm
n ⁺ -Ge	~10 ¹⁸ cm ⁻³	0.1 μm
n-Ge substrate		~300 μm
Metal		

Fig. 6 Schematic of the p-on-n Ge cell.

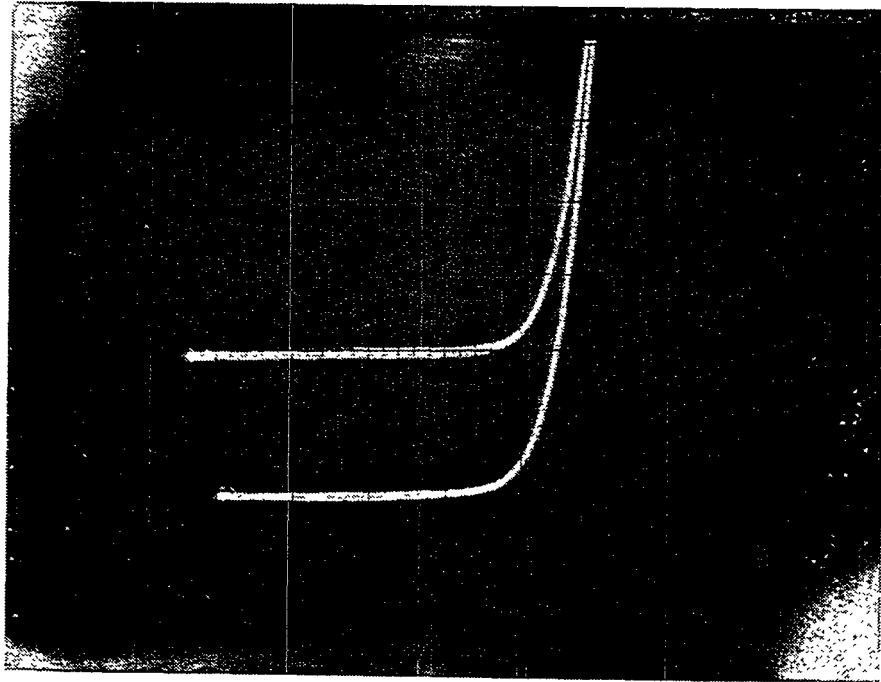


Fig. 7 Current-voltage curve for the p-on-n Ge device, a schematic of which is shown in Fig. 6. The x-axis scale is 0.1 volts/large division, and the y-axis scale is 2 mA/large division.

2.5 Development of the Cascade Structure

In developing the final cascade cell, a number of different structures were considered, both p-on-n and n-on-p structures grown on as-grown Ge junctions and on Ge junctions created by diffusion during the growth of the GaInAsP layers. Each type of structure will be discussed in turn.

2.5.1 Cascade Cells Grown on Active Ge Junctions

The first of the structures grown on active Ge junctions that we will consider has the p-on-n configuration. A schematic of the device structure is shown in Fig. 8. An n^{++} -GaInAsP layer was nucleated on a p^{++} -Ge layer, and then the subsequent GaInAsP layers were grown. The n^{++} -GaInAsP/ p^{++} -Ge structure within the device is meant to be the tunnel diode. A typical current-voltage curve (under AM 1.5D illumination) for one of a number of devices that was grown is shown in Fig. 9. The cell does have an anti-reflection (AR) coating. The V_{OC} for the device is 0.962 volts, the I_{SC} is 2.11 mA, and the fill factor is approximately 0.80. The active area of the device is 0.141 cm². Analysis of the device under GaAs filtered light gave no indication of a junction in the Ge. Under the GaAs filter, the GaInAsP junction is "turned off" except for leakage current. Any Ge junction would have a photoresponse to the filtered light, and would still be seen in the I-V curve. The p^{++} -Ge and the p^+ -Ge layers are lost during growth of the GaInAsP layer, apparently due to diffusion of As and P from the GaInAsP into the p-Ge layers, converting them to n-Ge. Even at growth temperatures of 675 °C, enough diffusion occurs during the overgrowth of the GaInAsP that the p-Ge layers are lost, and a p-on-n GaInAsP junction is left on n-Ge. Obviously, the n^{++} -GaInAsP/ p^{++} -Ge heterotunnel diode is not stable enough at 675 °C to remain intact after the growth of the GaInAsP. Because of the amount of time required to recalibrate compositions and doping concentrations at other temperatures, i.e., 650 °C, the decision was made to examine other cascade structures grown at 675 °C, rather than grow cascade cells at lower temperatures.

Metal		
p ⁺ -GaAs ~mid 10 ¹⁸ cm ⁻³ 0.2 μm		
p ⁺ -GaInP ₂	~10 ¹⁸ cm ⁻³	400 Å
p ⁺ -GaInAsP	1 x 10 ¹⁸ cm ⁻³	0.2 μm
n-GaInAsP	1 x 10 ¹⁷ cm ⁻³	3.5 μm
n ⁺ -AlInP ₂	1 x 10 ¹⁸ cm ⁻³	400 Å
n ⁺ -GaInAsP	1 x 10 ¹⁸ cm ⁻³	1.0 μm
n ⁺⁺ -GaInAsP	~10 ¹⁹ cm ⁻³	0.5 μm
p ⁺⁺ -Ge	~10 ¹⁹ cm ⁻³	0.1 μm
p ⁺ -Ge	1 x 10 ¹⁸ cm ⁻³	0.5 μm
n-Ge substrate		~300 μm
Metal		

Fig. 8 Schematic of the cascade cell that was grown on the p-on-n Ge junction.

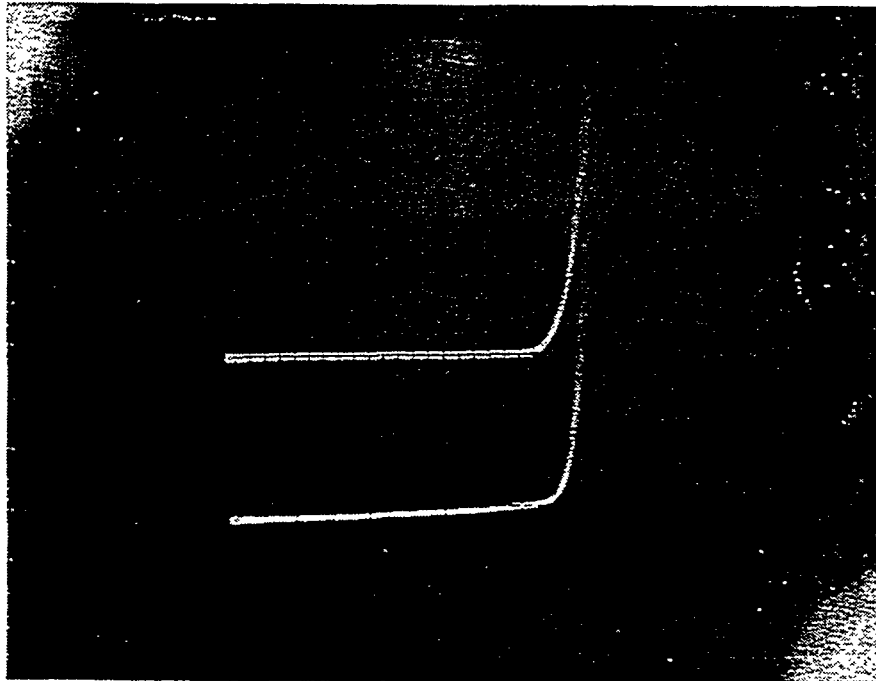


Fig. 9 Typical current-voltage curve for the type of cell shown in Fig. 8. The x-axis scale is 0.5 volts/large division, and the y-axis scale is 1.0 mA/large division.

The schematic for the cascade structure grown on n-on-p Ge junctions is shown in Fig. 10. Figs. 11 and 12 show typical current-voltage curves that are seen for these types of cells. V_{OC} s for a number of the cells are about 0.9 volts, and I_{SC} s are between 1 and 2 mA, for cells of area 0.141 cm^2 active area. Under illumination, a "kink" appears in the curve. The "kink" may be pronounced, as in Fig. 11, or it may be much smaller, as in Fig. 12. Examination of the cell under 6 suns concentration reveals a second "kink", one that is completely in the second quadrant. The second "kink" appears when the current-carrying limits of the tunnel diode are reached. Further increase in the magnitude of the concentrated light gives rise to the negative differential region of the tunnel diode being seen. The first "kink" seen in the I-V curves in Figs. 11 and 12 is not due to the tunnel diode, but is instead due to a poor quality junction in the Ge. During growth of the GaInAsP, the quality of the Ge junction degrades such that the Ge junctions have a very low reverse bias breakdown. The combination of the low breakdown voltage and current mismatch between the GaInAsP and Ge junctions leads to the type of "kink" seen in Figs. 11 and 12. The "soft knee" seen in the dark I-V curve in Fig. 11 is also due to the soft breakdown of the Ge junction. Even though n-on-p Ge junctions can be made that show good diode properties, e.g., Fig. 4, if these same junctions are held at $675 \text{ }^\circ\text{C}$ for growth of the GaInAsP layers, the Ge junctions deteriorate such that they cannot support a reverse voltage of any size.

Clearly, GaInAsP/Ge cascade cells cannot be made by the growth of GaInAsP layers on Ge junctions at $675 \text{ }^\circ\text{C}$. In the case of the p-on-n structure, the p-type emitter is lost due to diffusion of As and P into the emitter, while in the case of the n-on-p structure, the quality of the Ge junction deteriorates during growth of the GaInAsP layers.

Metal		
n ⁺ -GaAs ~mid 10 ¹⁸ cm ⁻³ 0.2 μm		
n ⁺ -AlInP ₂	~10 ¹⁸ cm ⁻³	250 Å
n ⁺ -GaInAsP	1 x 10 ¹⁸ cm ⁻³	0.2 μm
p-GaInAsP	1 x 10 ¹⁷ cm ⁻³	3.5 μm
p ⁺ -GaInP ₂	1 x 10 ¹⁸ cm ⁻³	400 Å
p-GaInAsP	1 x 10 ¹⁷ cm ⁻³	1.0 μm
p ⁺⁺ -GaInAsP	~10 ¹⁹ cm ⁻³	0.5 μm
n ⁺⁺ -GaInAsP	~10 ¹⁹ cm ⁻³	0.5 μm
n ⁺ -GaInAsP	~10 ¹⁸ cm ⁻³	3.5 μm
n ⁺⁺ -Ge	5 x 10 ¹⁸ cm ⁻³	0.1 μm
n ⁺ -Ge	1 x 10 ¹⁸ cm ⁻³	0.5 μm
p-Ge	1 x 10 ¹⁷ cm ⁻³	6.0 μm
p ⁺ -Ge	1 x 10 ¹⁸ cm ⁻³	0.1 μm
p-Ge substrate		~300 μm
Metal		

Fig. 10 Schematic of the cascade cell that was grown on the n-on-p Ge junction.

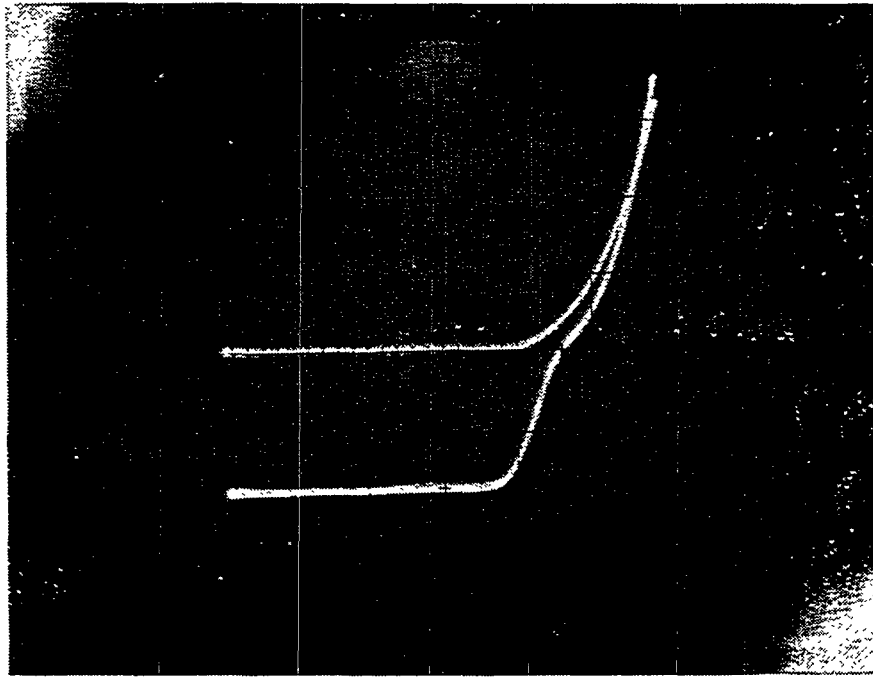


Fig. 11 Current-voltage curve for the structure grown in Fig. 10. The x-axis scale is 0.5 volts/large division, and the y-axis scale is 1.0 mA/large division.

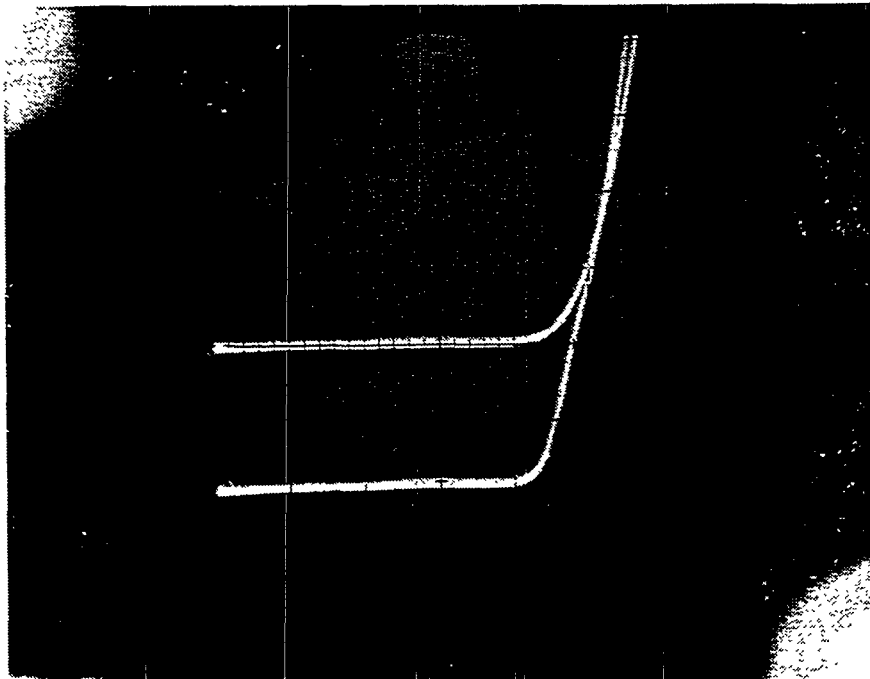


Fig. 12 Current-voltage curve of a second type for the structure shown in Fig. 10. The x-axis scale is 0.5 volts/large division, and the y-axis scale is 1 mA/large division.

2.5.2 Cascade Cells Grown with Diffused Ge Junctions

The results with the cascade devices grown at 675 °C on the Ge junctions led to considering growth of the GaInAsP layers at 675 °C on Ge substrates and having the Ge junction form by the diffusion of either Ga and In, or As and P into the Ge to create a junction. For example, the structure for a p-on-n cascade cell with a diffused Ge is shown in Fig. 13. The idea behind the device is to have Ga and In diffuse from an n⁺⁺-GaInAsP layer into the n-Ge at a higher solid solubility than As and P [1], hence creating both a p⁺⁺-Ge layer for an n⁺⁺-GaInAsP/p⁺⁺-Ge tunnel diode, and a p⁺-Ge layer for an emitter. Two different types of I-V curves are seen (Figs. 14 and 15) from devices grown in this manner. The first type of curve, Fig. 14, is similar to that shown in Fig. 11. Apparently, a poor quality junction is created in the Ge, one that has poor diode quality and also poor breakdown. The second type of curve, that of Fig. 15, has a very good I-V curve. The V_{OC} for the device shown is 1.06 volts, the I_{SC} is 2.4 mA, and the fill factor is 0.80. The device, with an active area of 0.141 cm², is illuminated with AM 1.5D light and does not have an AR coating. Further examination of the cell, however, does not indicate cascade action. As in the previous discussion on the use of GaAs filtered light, no evidence was seen for a junction in the Ge. Also, driving the cell with IR rich light gave no indication of a current mismatch in the I-V curve (which would indicate two junctions in the device). For a single junction, the V_{OC} is quite good, about equal to that seen for GaInAsP junctions grown on GaAs substrates. Apparently, for devices showing the second type of I-V curve, not enough diffusion of Ga and In into the n-Ge occurs at 675 °C to cause type conversion. It should be noted that both types of curves are seen in devices processed from the same wafer, the wafer being about 1 cm. by 2.5 cm. in size. Either not enough diffusion occurs to create the desired junction in the Ge, or if enough diffusion of Ga and In into the n-Ge occurs to type convert to p-type material, the junction created in the Ge is of too poor a quality to give good I-V curves.

Metal		
p ⁺ -GaAs ~mid 10 ¹⁸ cm ⁻³ 0.2 μm		
p ⁺ -GaInP ₂	~10 ¹⁸ cm ⁻³	400 Å
p ⁺ -GaInAsP	1 x 10 ¹⁸ cm ⁻³	0.2 μm
n-GaInAsP	1 x 10 ¹⁷ cm ⁻³	3.5 μm
n ⁺ -AlInP ₂	1 x 10 ¹⁸ cm ⁻³	400 Å
n ⁺ -GaInAsP	1 x 10 ¹⁸ cm ⁻³	1.0 μm
n ⁺⁺ -GaInAsP	~10 ¹⁹ cm ⁻³	0.5 μm
diffused p ⁺⁺ -Ge	~10 ¹⁹ cm ⁻³	250 Å
diffused p ⁺ -Ge	~10 ¹⁸ cm ⁻³	0.1 μm
n-Ge substrate		~300 μm
Metal		

Fig. 13 Schematic of the cascade cell that was grown on the n-type Ge substrate.

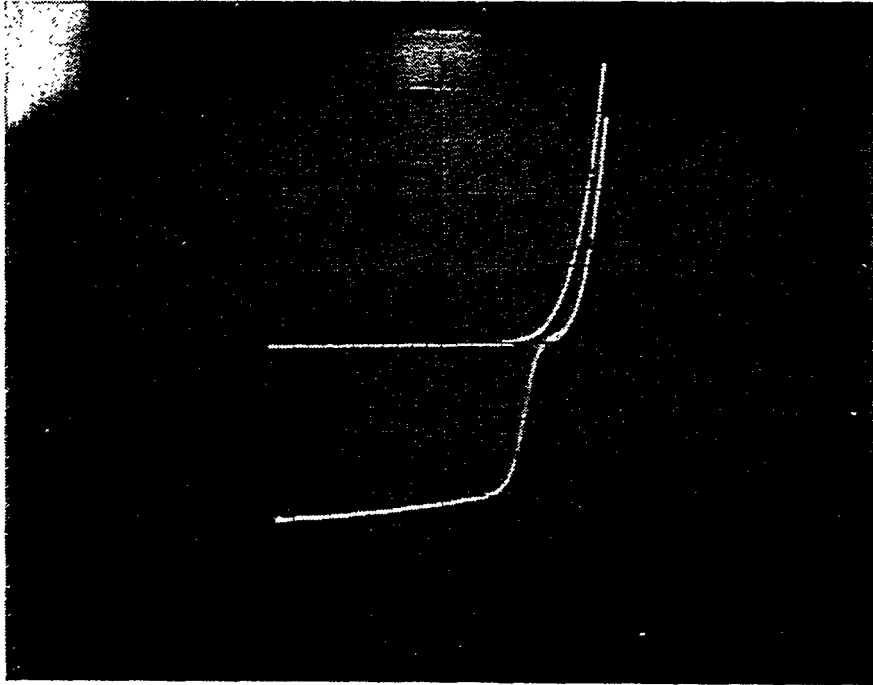


Fig. 14 Current-voltage curve for the structure grown in Fig. 13. The x-axis scale is 0.5 volts/large division, and the y-axis scale is 1 mA/large division.

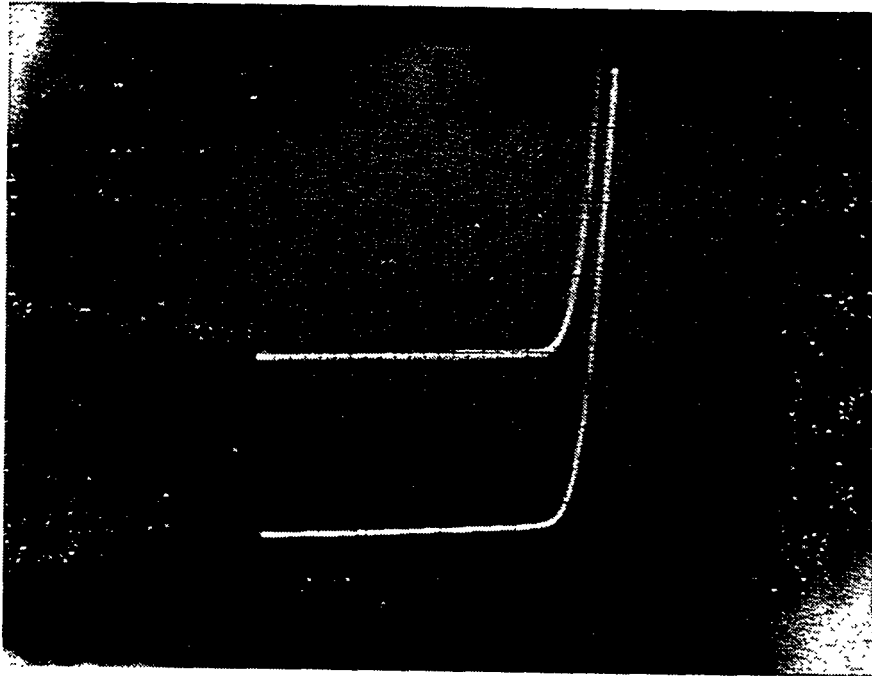


Fig. 15 Current-voltage curve of a second type for the structure grown in Fig. 13. The x-axis scale is 0.5 volts/large division, and the y-axis scale is 1 mA/large division.

The difficulty in trying to create a diffused p-on-n Ge junction is that so much As and P have already diffused in, once the Ga and In diffuse in in sufficient quantities, the doping levels on both sides of the junction are so high that the junction is of poor quality.

Fig. 16 shows a schematic of the n-on-p cascade structure with a diffused Ge junction. This is the only structure that we grew that demonstrated cascade action. Both a GaInAsP tunnel diode and a GaInAsP solar cell are grown on a p-Ge substrate. During growth of the GaInAsP layers, As and P diffuses into the p-Ge, type converting it to n-Ge, and thus creating a junction in the Ge. The I-V curve for the best cell that has been grown is shown in Fig. 17. Under AM 1.5D illumination, with an AR coating, the V_{oc} is 1.18 volts, the I_{sc} is 2.59 mA, and the fill factor is 0.75. The active area of the device is 0.141 cm^2 , and the active area efficiency is 16.2%.

We have had however, difficulty in duplicating the device shown in Fig. 16. Despite a number of growth attempts, we have only had a yield of about 7.5%. Not only do results vary from run to run, but devices processed from the same wafer may vary, with some cells showing cascade action, and some not showing any cascade action. Several factors contribute to the low yield and lack of repeatability. First, the doping in the p-Ge must be low enough such that type conversion due to the indiffusion of As and P occurs. If the doping in the p-Ge is too high, type conversion will not occur, and a poor quality junction remains at the n^+ -GaInAsP/p-Ge interface. Secondly, if a diffused junction is created in the Ge, it still must be of reasonable quality. Poor quality junctions in the Ge lead to the types of I-V curves seen in Figs. 14 and 10. Finally, the issues of lattice-matching, discussed in Section 2.3, must be addressed. If the lattice-matching between the GaInAsP and the Ge is not exact, bowing of the wafers is seen. The thicker the GaInAsP layers, the more stringent are the requirements on the lattice-matching. During growths of the structure shown in Fig. 16, slight variations in the composition changed the bowing in the wafers from convex to concave. Despite these difficulties, we believe that, with further work, the GaInAsP/Ge cascade cell can be further improved.

Metal		
n ⁺ -GaAs ~mid 10 ¹⁸ cm ⁻³ 0.2 μm		
n ⁺ -AlInP ₂	~10 ¹⁸ cm ⁻³	400 Å
n ⁺ -GaInAsP	1 x 10 ¹⁸ cm ⁻³	0.2 μm
p-GaInAsP	1 x 10 ¹⁷ cm ⁻³	3.5 μm
p ⁺ -GaInP ₂	1 x 10 ¹⁸ cm ⁻³	400 Å
p ⁺⁺ -GaInAsP	~10 ¹⁹ cm ⁻³	0.5 μm
n ⁺⁺ -GaInAsP	~10 ¹⁹ cm ⁻³	0.5 μm
n ⁺ -GaInAsP	1 x 10 ¹⁸ cm ⁻³	1.5 μm
diffused n ⁺ -Ge	~10 ¹⁸ cm ⁻³	0.1 μm
p-Ge substrate		~300 μm
Metal		

Fig. 16 Schematic of the cascade cell that was grown on the p-type Ge substrate.

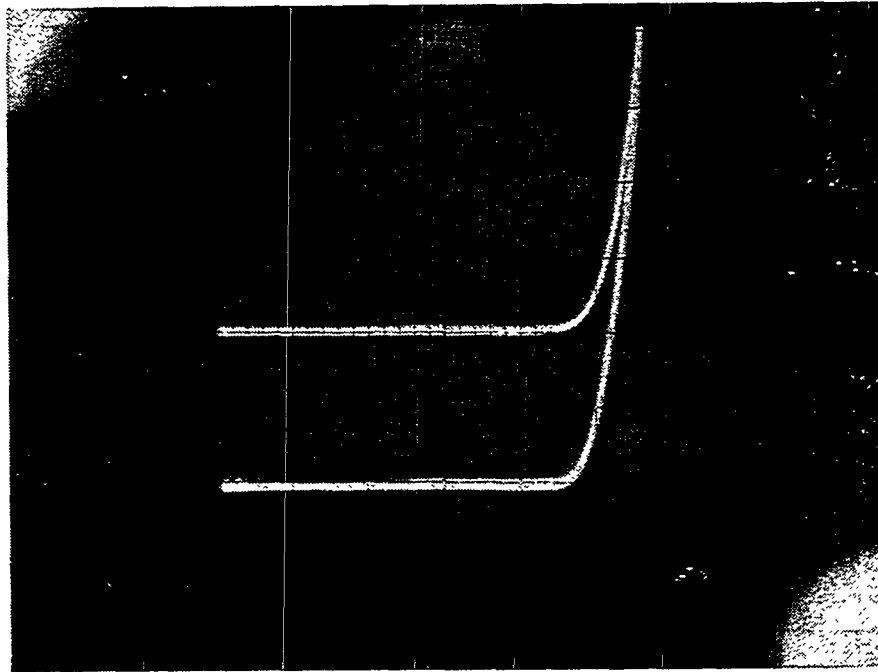


Fig. 17 Current-voltage curve for the structure shown in Fig. 16. The x-axis scale is 0.5 volts/large division, and the y-axis scale is 1 mA/large division.

3.0 Summary and Closing Comments

Overall, several significant accomplishments have been made during the three years of this work. They include:

1. growth of GaInAsP with minority carrier lifetimes of 35 ns and 3.7 ns in n-type and p-type material, respectively,
2. fabrication of an n-on-p GaInAsP cell on GaAs with a 1 sun active-area efficiency of 21.8% and a 10 sun active-area efficiency of 23.4%, and
3. demonstration of an n-on-p GaInAsP/Ge cascade cell with an active-area efficiency of 16.2%.

In view of the accomplishments of the past three years, we feel that the program has been a success. A number of challenges remain in order to approach the theoretical efficiencies that are possible with the GaInAsP/Ge cascade cell. With further effort, we feel that these challenges can be overcome, and so improving the GaInAsP/Ge is worth pursuing.

4.0 References

1. Final Report for Contract WL-TR-91-2096, Aero Propulsion & Power Directorate, Wright Laboratory, Wright Patterson Air Force Base, Ohio 45433-6563
2. R. Venkatasubramanian, M. L. Timmons, T. S. Colpitts, and S. Asher, **J. Elect. Mat'ls.** **21**, 1992, 893.

5.0 Appendix

The following is a copy of a paper presented at the IEEE PV Specialists Conference in Louisville, KY, in May, 1993.

DEVELOPMENT OF 20% EFFICIENT GaInAsP SOLAR CELLS

P. R. Sharps, M. L. Timmons, R. Venkatasubramanian, R. Pickett, J. S. Hills, J. Hancock, and J. Hutchby
Research Triangle Institute, Research Triangle Park, NC 27709.

P. Iles and C. L. Chu
Applied Solar Energy Corp., City of Industry, CA 91749

M. Wanlass and J. S. Ward
National Renewable Energy Laboratory, Golden, CO 80401

ABSTRACT

We report on the development of two compositions of GaInAsP lattice-matched to GaAs for photovoltaic applications. Successful development of cascade solar cells necessitates the development of both high bandgap (1.5 to 1.9 eV) as well as low bandgap (0.7 to 1.4 eV) materials. GaInAsP lattice-matched to GaAs is an excellent candidate for the high band gap material. $\text{Ga}_{0.84}\text{In}_{0.16}\text{As}_{0.68}\text{P}_{0.32}$ cells, with a band gap of 1.55 eV, have been developed that have demonstrated a V_{oc} of 1.047 volts, a J_{sc} of 22.5 mA/cm², a fill factor of 0.849, and an active area efficiency of 21.8 per cent under AM1.5 direct illumination. A $\text{Ga}_{0.84}\text{In}_{0.16}\text{As}_{0.68}\text{P}_{0.32}$ tunnel diode has also been developed with a peak current of $4.33 \times 10^2 \sim \text{mA/cm}^2$ at a voltage of 65 mV. Both the $\text{Ga}_{0.84}\text{In}_{0.16}\text{As}_{0.68}\text{P}_{0.32}$ cell and tunnel diode are being used in conjunction with a Ge cell to develop a monolithic $\text{Ga}_{0.84}\text{In}_{0.16}\text{As}_{0.68}\text{P}_{0.32}/\text{Ge}$ cascade cell. $\text{Ga}_{0.68}\text{In}_{0.32}\text{As}_{0.34}\text{P}_{0.66}$ cells, with a band gap of 1.7 eV, have been developed that have demonstrated a V_{oc} of 1.161 volts, a J_{sc} of 28.9 mA/cm², a fill factor of 0.86, and an active area efficiency of 21.4 per cent under AM0 illumination. The $\text{Ga}_{0.68}\text{In}_{0.32}\text{As}_{0.34}\text{P}_{0.66}$ cells have also demonstrated resistance to radiation damage as well as a recovery of preirradiation performance after low temperature annealing.

INTRODUCTION

Cascade solar cells have already demonstrated highly efficient conversion of sunlight into electricity. The GaAs/GaSb and the GaAs/GaInAsP mechanically stacked cascade cells have shown efficiencies greater than 30 per cent under concentration [1,2]. A three-terminal InP/GaInAs₂ monolithic cascade cell has demonstrated an efficiency greater than 30 per cent under concentration [2], and a two-terminal GaInP₂/GaAs monolithic cascade cell has shown an efficiency of 27.3 per cent at one sun [3].

A number of different materials combinations have been suggested for both monolithic and mechanically stacked

cascade cells. The work of Wanlass et al. [2] has indicated that the cascade cells with the highest theoretical efficiencies have IR-sensitive bottom junctions with bandgaps in the range from 0.7 to 1.1 eV. For monolithic cascade cells, the challenge is to have two photovoltaic junctions of separate materials that will both current match as well as lattice match, and to also develop a suitable lattice-matched tunnel diode interconnect between the two junctions. For series-connected mechanically stacked cascade cells, the challenge is to develop two photovoltaic junctions of different materials that current match, to grow the top junction on a removable substrate, and to develop a suitable electrical interconnect between the two junctions.

Quaternary semiconductor compounds are ideal candidates for use in cascade solar cells because the lattice constant and the bandgap of such compounds can be, within limits, independently varied. For GaInAsP lattice-matched to GaAs (and, hence, Ge), the bandgap spans the range from 1.42 to 1.92 eV (Fig. 1). The lattice constant and bandgap of GaInAsP compositions are easily measured by x-ray diffraction and photoluminescence measurements. Two compositions of GaInAsP lattice-matched to GaAs are of particular interest in the present study. Junctions made from $\text{Ga}_{0.84}\text{In}_{0.16}\text{As}_{0.68}\text{P}_{0.32}$, with a bandgap of 1.55 eV, are both current-matched and lattice-matched with Ge junctions. Under concentrated sunlight, a $\text{Ga}_{0.84}\text{In}_{0.16}\text{As}_{0.68}\text{P}_{0.32}/\text{Ge}$ cascade cell projects to a theoretical efficiency of greater than 40 per cent at 100 suns [2]. Such cells are of interest for terrestrial applications. The composition $\text{Ga}_{0.68}\text{In}_{0.32}\text{As}_{0.34}\text{P}_{0.66}$ has a bandgap of 1.7 eV, and junctions made from such a material are current-matched with Si junctions. By growing on a removable Ge substrate, the $\text{Ga}_{0.68}\text{In}_{0.32}\text{As}_{0.34}\text{P}_{0.66}$ junction can be mechanically stacked on a Si junction. The $\text{Ga}_{0.68}\text{In}_{0.32}\text{As}_{0.34}\text{P}_{0.66}/\text{Si}$ mechanically stacked cell also projects to a theoretical efficiency of greater than 40 per cent at 100 suns [2], and is of interest for space applications.

GaInAsP cells of both compositions are grown at RTI in a vertical, atmospheric-pressure, organometallic vapor phase

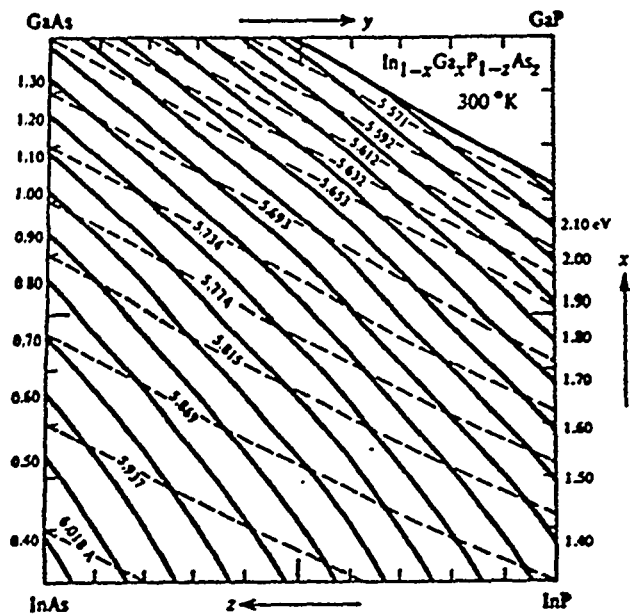


Fig. 1. The variation in the bandgap and the lattice constant in GaInAsP at room temperature [6].

epitaxy (OMVPE) reactor at 675 °C. Trimethylgallium (TMGa), ethyldimethylindium (EDMIIn), trimethylaluminum (TMAI), 100% arsine, and 100% phosphine are the precursors. Diethylzinc (DEZn) is used to supply the p-type dopant, and a 50 ppm H₂Se in H₂ mixture is used to supply the n-type dopant.

DEVELOPMENT OF THE Ga_{0.84}In_{0.16}As_{0.68}P_{0.32} CELL

A number of Ga_{0.84}In_{0.16}As_{0.68}P_{0.32} cells with either an n-on-p or p-on-n configuration have been grown and processed at RTI. A schematic of a cell with an n-on-p configuration is shown in Fig. 2. The cells are 0.16 cm² in total area, with an active area of 0.136 cm². Results to date for a number of cells indicate that the n-on-p configuration gives better efficiencies than the p-on-n configuration. The V_{oc} for either configuration is about the same; the major difference is in the J_{sc}, with the current for the n-on-p configuration being about 25 per cent higher than that for the p-on-n configuration. This is believed to be due to the longer diffusion lengths of minority carriers in p-type material as compared to n-type material.

For the n-on-p configuration, Al_{0.8}Ga_{0.2}As, AlInP₂, and GaInP₂ have been considered as window materials. Growth of high quality AlGaAs with an aluminum content greater than 50% is difficult with our current reactor configuration. Since AlInP₂ has a larger bandgap (2.3 eV) than GaInP₂ (1.9 eV), the AlInP₂ window will help to improve the blue response of the cell. Due to the difficulty in obtaining low resistivity p-AlInP₂

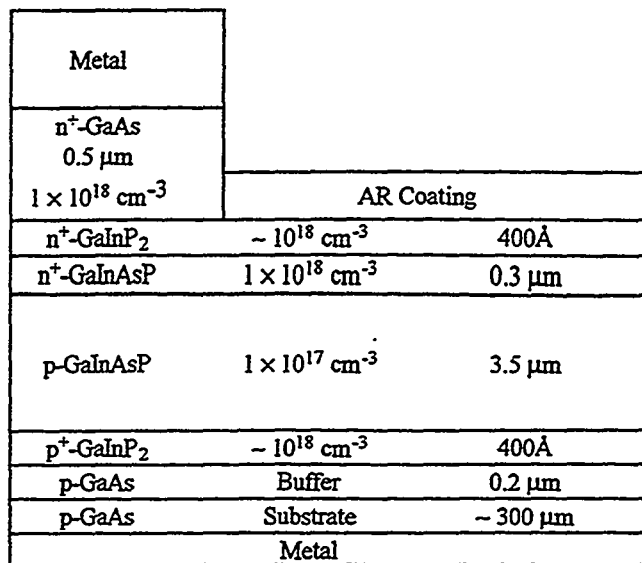


Fig. 2. Schematic of a Ga_{0.84}In_{0.16}As_{0.68}P_{0.32} cell with an n-on-p configuration.

at 675°C, GaInP₂ is used to create the back surface field (BSF) for the n-on-p cells.

The best Ga_{0.84}In_{0.16}As_{0.68}P_{0.32} cell to date, grown on p-GaAs, has a V_{oc} of 1.047 volts, a J_{sc} of 22.5 mA/cm², a fill factor of 0.849, an active area efficiency of 21.8 per cent for AM1.5 direct illumination (Fig. 3), and an active area efficiency of 23.4 per cent under 9.73 suns. (Active area efficiencies are given because of the 15% grid coverage and because the cells are designed for use with cover glasses). As far as we know, this is the highest efficiency ever demonstrated for a quaternary cell under AM1.5 illumination. A spectral response measurement for the cell is shown in Fig. 4. The longer wavelength cut-off corresponds well with the bandgap of 1.55 eV, and is also fairly sharp, indicating a good minority carrier diffusion length. There is some current loss at shorter wavelengths, possibly due to the thickness of the emitter (0.3 μm) or to the GaInP₂ window. Since the cells are designed for concentrator applications, the emitter thickness is constrained by the need to keep the series resistance low. Switching to an AlInP₂ window should help with the blue response.

A number of Ga_{0.84}In_{0.16}As_{0.68}P_{0.32} solar cells grown at RTI have been processed at the National Renewable Energy Laboratory (NREL). Fig. 5 shows the results for a cell without an anti-reflection (AR) coating, measured at 69 suns. The total area efficiency is 15.7%. Addition of an AR coating will increase the efficiency approximately 30%, to give a total area efficiency of about 20.8%. Fig. 6 shows the log current-voltage curve for another cell. The modeled shunt resistance is 1.9 × 10⁶ Ω-cm², and the series resistance is 3.8 × 10⁻¹

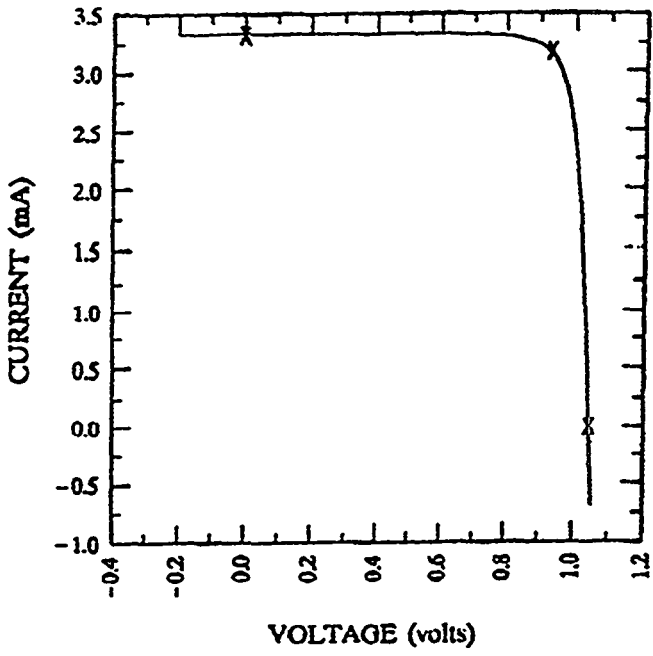


Fig. 3. Current-voltage curve for the n-on-p $\text{Ga}_{0.84}\text{In}_{0.16}\text{As}_{0.68}\text{P}_{0.32}$ cell on GaAs, under AM1.5 direct illumination. The active area efficiency is 21.8%.

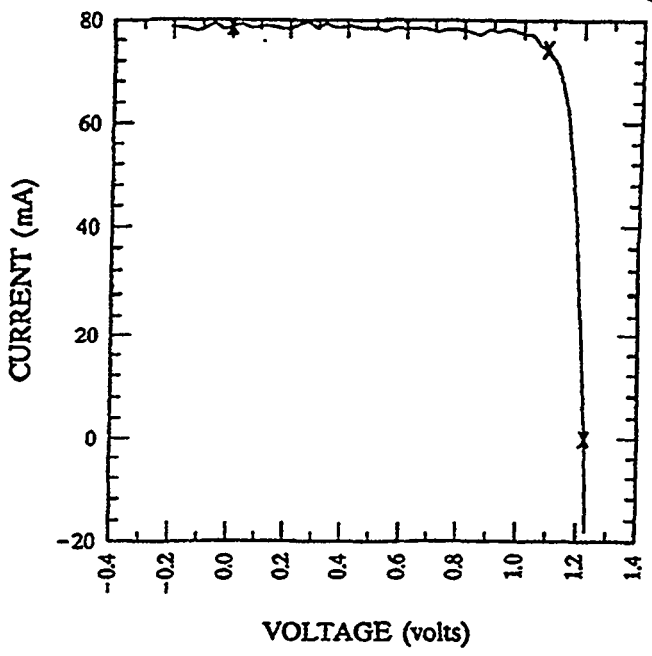


Fig. 5. Current-voltage curve for an n-on-p $\text{Ga}_{0.84}\text{In}_{0.16}\text{As}_{0.68}\text{P}_{0.32}$ cell at 69 suns.

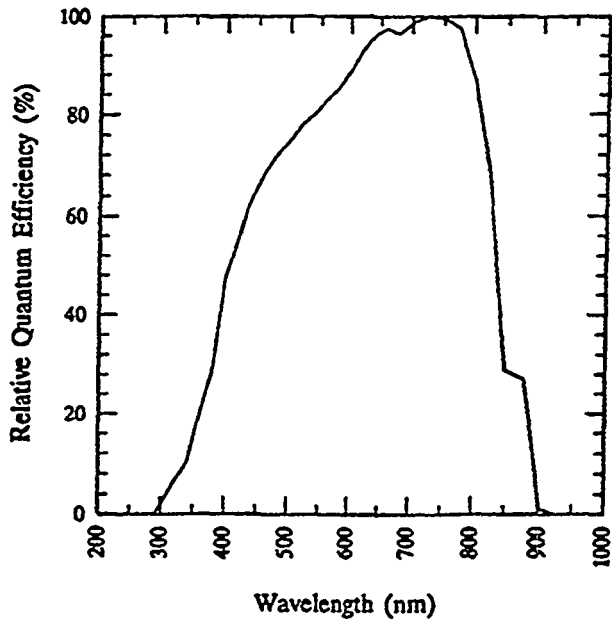


Fig. 4. Spectral response curve for the n-on-p $\text{Ga}_{0.84}\text{In}_{0.16}\text{As}_{0.68}\text{P}_{0.32}$ cell on GaAs.

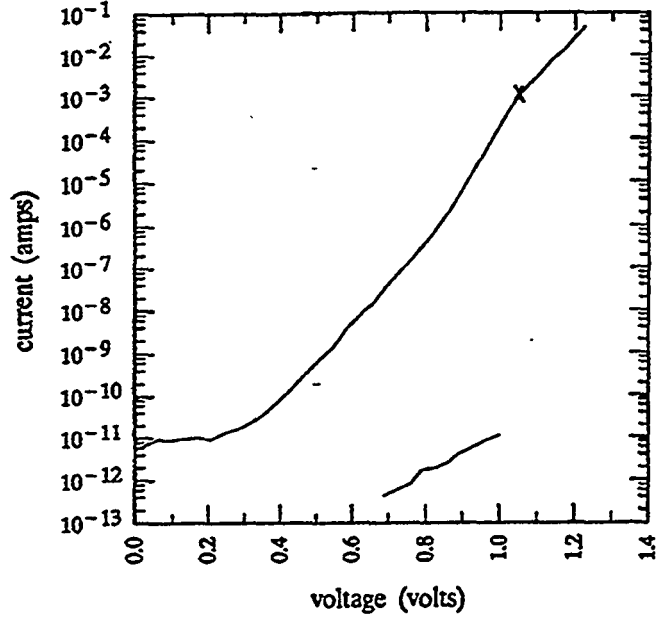


Fig. 6. Log current-voltage curve for an n-on-p $\text{Ga}_{0.84}\text{In}_{0.16}\text{As}_{0.68}\text{P}_{0.32}$ cell on GaAs.

\sim ohm-cm². The results indicate that the $\text{Ga}_{0.84}\text{In}_{0.16}\text{As}_{0.68}\text{P}_{0.32}$ cell can operate up to 69 suns with high fill factors.

Since the ultimate goal of the research in $\text{Ga}_{0.84}\text{In}_{0.16}\text{As}_{0.68}\text{P}_{0.32}$ is to develop a $\text{Ga}_{0.84}\text{In}_{0.16}\text{As}_{0.68}\text{P}_{0.32}/\text{Ge}$ cascade cell, an appropriate tunnel junction interconnect has to be developed. The logical choice

is $\text{Ga}_{0.84}\text{In}_{0.16}\text{As}_{0.68}\text{P}_{0.32}$, since the material is lattice-matched to Ge and is also optically transparent to photons that would normally be collected by the bottom cell. A current-voltage curve for a p^{++}/n^{++} $\text{Ga}_{0.84}\text{In}_{0.16}\text{As}_{0.68}\text{P}_{0.32}$ tunnel diode, nucleated directly on Ge, is shown in (approximately what the $\text{Ga}_{0.84}\text{In}_{0.16}\text{As}_{0.68}\text{P}_{0.32}/\text{Ge}$ cascade cell would produce under 10 suns), the voltage drop across the tunnel diode is 4.5 mV. Under 100 suns, the voltage drop would be 45 mV. The

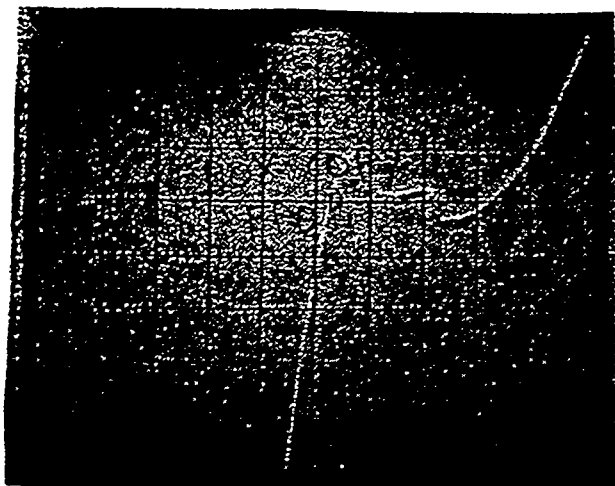


Fig. 7. The peak current for the device is $4.3 \times 10^3 \sim \text{mA/cm}^2$, and occurs at a voltage of 65 mV. For a current density of 300 mA/cm^2 Fig. 7 Current-voltage curve for a $p^{++}\text{-}n^{++} \text{Ga}_{0.84}\text{In}_{0.16}\text{As}_{0.68}\text{P}_{0.32}$ tunnel diode nucleated directly on Ge. The x-axis scale is 0.1V per large division, and the y-axis scale is 2 mA per division. the area of the tunnel diode is $9 \times 10^{-4} \text{ cm}^2$.

"kink" in the negative resistance region is believed to be due to tunneling occurring between the degenerate bands and a deep level within the bandgap. The fact that $\text{Ga}_{0.84}\text{In}_{0.16}\text{As}_{0.68}\text{P}_{0.32}$ can be nucleated directly on Ge indicates that the complete monolithic cascade structure can be grown without the need for a separate material to act as a buffer layer (such as GaAs) between $\text{Ga}_{0.84}\text{In}_{0.16}\text{As}_{0.68}\text{P}_{0.32}$ and Ge.

Research is currently underway to optimize the Ge bottom cell (grown by vapor phase epitaxy) and to also grow the complete monolithic structure using $\text{Ga}_{0.84}\text{In}_{0.16}\text{As}_{0.68}\text{P}_{0.32}$ as the tunnel diode. Fig. 8 gives a schematic of a possible $\text{Ga}_{0.84}\text{In}_{0.16}\text{As}_{0.68}\text{P}_{0.32}/\text{Ge}$ cascade cell.

DEVELOPMENT OF THE $\text{Ga}_{0.68}\text{In}_{0.32}\text{As}_{0.34}\text{P}_{0.66}$ SOLAR CELL

The development of the $\text{Ga}_{0.68}\text{In}_{0.32}\text{As}_{0.34}\text{P}_{0.66}$ solar cell is motivated by the desire to find a material with a bandgap in the 1.7 eV range that does not have the same stringent growth requirements as AlGaAs. High quality AlGaAs for photovoltaic applications requires high growth temperatures ($>750^\circ\text{C}$), ultra-clean growth systems, and very pure sources.. The growth of high quality $\text{Ga}_{0.68}\text{In}_{0.32}\text{As}_{0.34}\text{P}_{0.66}$ is not as

Metal		
$n^+\text{-GaAs}$ 0.5 μm $1 \times 10^{18} \text{ cm}^{-3}$		AR Coating
$n^+\text{-AlInP}_2$	$\sim 10^{18} \text{ cm}^{-3}$	400Å
$n^+\text{-GaInAsP}$	$1 \times 10^{18} \text{ cm}^{-3}$	0.3 μm
$p\text{-GaInAsP}$	$1 \times 10^{17} \text{ cm}^{-3}$	3.5 μm
$p^+\text{-GaInP}_2$	$\sim 10^{18} \text{ cm}^{-3}$	400Å
$p^{++}\text{-GaInP}$	$\sim 10^{19} \text{ cm}^{-3}$	0.5 μm
$n^{++}\text{-GaInP}$	$\sim 10^{19} \text{ cm}^{-3}$	0.5 μm
$n^+\text{-GaInAsP}$	$1 \times 10^{18} \text{ cm}^{-3}$	3.5 μm
$n^+\text{-Ge}$	$1 \times 10^{18} \text{ cm}^{-3}$	1.0 μm
$p\text{-Ge}$	$1 \times 10^{17} \text{ cm}^{-3}$	6.0 μm
$p\text{-Ge}$	Substrate	$\sim 300 \mu\text{m}$
	Metal	

Fig. 8. Schematic of the $\text{Ga}_{0.84}\text{In}_{0.16}\text{As}_{0.68}\text{P}_{0.32}/\text{Ge}$ cascade cell.

difficult. The most difficult aspect of growing $\text{Ga}_{0.68}\text{In}_{0.32}\text{As}_{0.34}\text{P}_{0.66}$, when using AsH_3 and PH_3 as the precursors, is the temperature differential in the decomposition temperatures of PH_3 and AsH_3 . AsH_3 decomposes at a lower temperature than PH_3 [4]. For GaInAsP compositions such as $\text{Ga}_{0.68}\text{In}_{0.32}\text{As}_{0.34}\text{P}_{0.66}$, with a high phosphorus content, considerably more PH_3 than AsH_3 is required to achieve the desired composition. However, new precursors, such as tertiary-butyl phosphine (TBP), have lower cracking temperatures than PH_3 , and are an obvious alternative for the growth of $\text{Ga}_{0.68}\text{In}_{0.32}\text{As}_{0.34}\text{P}_{0.66}$. Future research plans include using TBP for the growth of the quaternary.

The ultimate goal of the research into $\text{Ga}_{0.68}\text{In}_{0.32}\text{As}_{0.34}\text{P}_{0.66}$ is the development of a cell that can be mechanically stacked with a Si cell for use in a cascade structure. A schematic of an n-on-p $\text{Ga}_{0.68}\text{In}_{0.32}\text{As}_{0.34}\text{P}_{0.66}$ cell is shown in Fig. 9. The n-on-p configuration is chosen again because of the longer minority carrier diffusion length in p-type as compared to n-type material, and also because of the difficulty in growing a low resistivity p-type AlInP₂ window. Results for efficiency, radiation resistance, and recovery from radiation damage for the cells indicate that

Metal		
n ⁺ -GaAs	0.5 μm	
1 × 10 ¹⁸ cm ⁻³		AR Coating
n ⁺ -AlInP ₂	~ 10 ¹⁸ cm ⁻³	400Å
n ⁺ -GaInAsP	1 × 10 ¹⁸ cm ⁻³	0.1 μm
p-GaInAsP	1 × 10 ¹⁷ cm ⁻³	3.5 μm
p ⁺ -GaInAsP	~ 10 ¹⁸ cm ⁻³	400Å
p ⁺ -GaInAsP ₂	~ 10 ¹⁹ cm ⁻³	400Å
p ⁺ -GaAs	~ 10 ¹⁹ cm ⁻³	400Å
p ⁺ -GaAs	1 × 10 ¹⁸ cm ⁻³	0.2 μm
p-GaAs	Substrate	~ 300 μm
		Metal

Fig. 9. Schematic of the n-on-p Ga_{0.68}In_{0.32}As_{0.34}P_{0.66} cell.

Ga_{0.68}In_{0.32}As_{0.34}P_{0.66} is an outstanding material for solar cell applications.

To date, all cells have been grown on GaAs. Fig. 10 shows the I-V curve for the best cell. The total area of the cell is 0.16 cm². Under AM0 illumination, the V_{oc} is 1.161 V, the J_{sc} is 28.9 mA/cm², the fill factor is 0.86, and the active area efficiency is 21.6 per cent. The active area efficiency again is given because the cell has a grid obscuration of 15 per cent. As far as we know, this is the highest efficiency ever demonstrated for a quaternary cell under AM0 illumination.

Spectral response measurements of the cell before and after irradiation with 1 MeV electrons at a fluence of 10¹⁵ ~ cm⁻² are shown in Fig. 11. Table I gives the average data for 7 cells before and after irradiation, and also shows the recovery of preirradiation performance with low temperature annealing. The EOL/BOL ratio, measured just after irradiation, is 0.79, but recovers to 0.84. The improvement in radiation damage occurs while the cells are held at room temperature. As far as we know, these are the first epitaxial films to demonstrate such recovery from radiation damage.

By way of comparison, results for the Ga_{0.68}In_{0.32}As_{0.34}P_{0.66} cell are compared with those for an Al_{0.2}Ga_{0.8}As cell, a material with the same nominal bandgap, in Table II. The V_{oc} for the Al_{0.2}Ga_{0.8}As cell is about 5 per cent higher, but the J_{sc} for the Ga_{0.68}In_{0.32}As_{0.34}P_{0.66} cell is about 21 per cent larger, taking into account the bandgap difference. The minority carrier diffusion length of the Ga_{0.68}In_{0.32}As_{0.34}P_{0.66} is an excellent alternative to Al_{0.2}Ga_{0.8}As since it has approximately

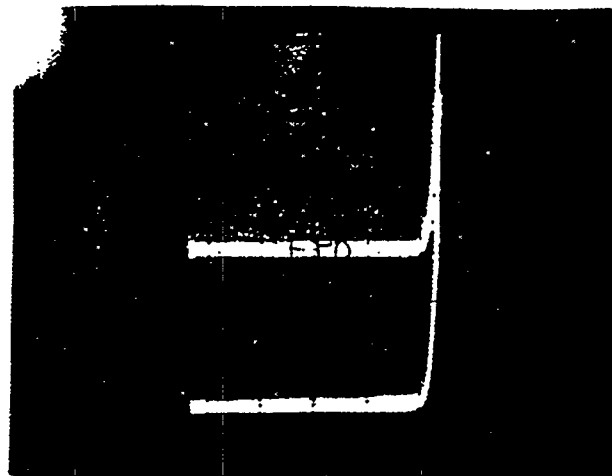


Fig. 10. Current-voltage curve for the best n-on-p Ga_{0.68}In_{0.32}As_{0.34}P_{0.66} cell to date. The x-axis scale is 0.5 V per large division, and the y-axis scale is 1 mA per division.

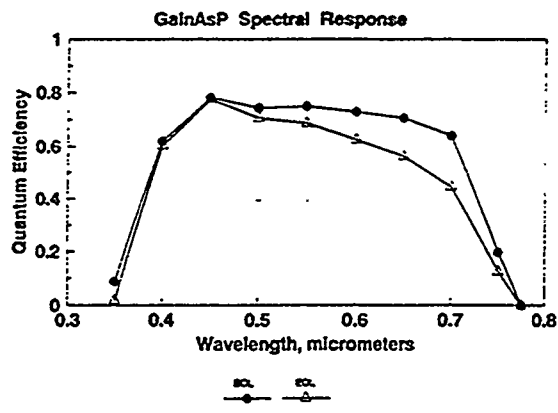


Fig. 11. Spectral response measurements for the Ga_{0.68}In_{0.32}As_{0.34}P_{0.66} cell before and after irradiation with 1 MeV electrons at a fluence of 10¹⁵ cm⁻².

the same bandgap, gives a higher efficiency for photovoltaic cells, and is grown apparently much better than that for the Al_{0.2}Ga_{0.8}As. The about 100°C lower than the Al_{0.2}Ga_{0.8}As.

The efficiencies, radiation resistance, and recovery from radiation for Ga_{0.68}In_{0.32}As_{0.34}P_{0.66} cells indicate that it is an outstanding material for space photovoltaic applications. Since the material is lattice-matched to GaAs, it is also lattice-matched to Ge and can be grown on Ge with the appropriate buffer. With the removal of the Ge substrate [5] and the use of an appropriate bonding technique, the Ga_{0.68}In_{0.32}As_{0.34}P_{0.66} cell can be stacked on Si cells for the development of a cascade structure.

Table 1. Average I-V Data for 7 GaInAsP Solar Cells Before and After Irradiation with 1 MeV Electrons at a Fluence of 10^{15} cm^{-2} Showing Recovery of Preirradiation Performance With Low-Temperature Annealing

CELL NO.	V_{oc0}	V_{oc1}	V_{oc2}	V_{oc3}	I_{sc0}	I_{sc1}	I_{sc2}	I_{sc3}	E_{ff0}	E_{ff1}	E_{ff2}	E_{ff3}
		(mV)				(mA)				(%)		
AVG.	1162	1096	1114	1122	3.76	3.25	3.30	3.36	20.4	16.1	16.7	17.2

NOTES: V_{oc0} , I_{sc0} , and E_{ff0} are preirradiation values.
 V_{oc1} , I_{sc1} , and E_{ff1} are values measured immediately after irradiation.
 V_{oc2} , I_{sc2} , and E_{ff2} were measured after 3-week storage in dry box at room temperature.
 V_{oc3} , I_{sc3} , and E_{ff3} were measured after 16 hours under AM0 spectrum (from Hoffmann simulator) at 28 °C after 3-week storage.

Table 2. Comparison of GaInAsP and AlGaAs Solar Cells

	AlGaAs	GaInAsP
V_{oc}	1215 mV	1161 mV
J_{sc}	21.9 mA/cm ²	28.9 mA/cm ²
ff	0.865	0.86
η , %	17.1	21.6

The cells were measured under AM0 light from a Hoffman simulator. The efficiencies refer to the active area.

CONCLUSIONS

Both compositions of GaInAsP that we have examined have demonstrated solar cells with active area efficiencies greater than 21 per cent. For terrestrial applications $\text{Ga}_{0.84}\text{In}_{0.16}\text{As}_{0.68}\text{P}_{0.32}$, in conjunction with a Ge cell, is an excellent candidate for a high efficiency, monolithic cascade cell. For space applications $\text{Ga}_{0.68}\text{In}_{0.32}\text{As}_{0.34}\text{P}_{0.66}$ has demonstrated good radiation resistance as well as recovery from radiation damage in addition to high efficiencies.

ACKNOWLEDGMENTS

This research has been supported by the National Renewable Energy Laboratory, Golden, CO 80401, under Subcontract No. XM-0-19142-3 and by the United States Air Force Material Command, Phillips Laboratory (PL), Kirtland AFB, NM 87117-6008, under Contract No. F33615-91-C-21155. Mr. J. Benner and Lt. K. Gledhill are the NREL Contract Monitor and the Air Force Project Engineer, respectively.

REFERENCES

- [1] L. M. Fraas, J. E. Avery, Y. S. Sundaram, V. T. Dinh, J. M. Gee, and K. A. Emery, *Proc. 21st IEEE Photovoltaic Specialists Conf.*, IEEE, New York, 1990, pp. 190.
- [2] M. W. Wanlass, J. S. Ward, K. A. Emery, T. A. Gessert, C. R. Osterwald, and T. J. Coutts, *Solar Cells* 30 (1991), pp. 363.
- [3] N. M. Olson, S. R. Kurtz, A. E. Kibbler, and P. Faine, *Appl. Phys. Lett.* 56 (1990), pp. 623.
- [4] G. B. Stringfellow, *Organometallic Vapor-Phase Epitaxy: Theory and Practice*, Academic Press, New York, 1989.
- [5] R. Venkatasubramanian, M. L. Timmons, and T. S. Colpitts, *Appl. Phys. Lett.* 59 (1991), pp. 2153.
- [6] G. E. Stillman, L. W. Cook, N. Tabatabaie, G. E. Bullman, and V. M. Robbins, *IEEE Trans. Elect. Dev.*, ED-40, (1983), pp. 364.

REPORT DOCUMENTATION PAGE

Form Approved
OMB NO. 0704-0188

Public reporting burden for this collection of information is estimated to average 1 hour per response, including the time for reviewing instructions, searching existing data sources, gathering and maintaining the data needed, and completing and reviewing the collection of information. Send comments regarding this burden estimate or any other aspect of this collection of information, including suggestions for reducing this burden, to Washington Headquarters Services, Directorate for Information Operations and Reports, 1215 Jefferson Davis Highway, Suite 1204, Arlington, VA 22202-4302, and to the Office of Management and Budget, Paperwork Reduction Project (0704-0188), Washington, DC 20503.

1. AGENCY USE ONLY (Leave blank)	2. REPORT DATE October 1994	3. REPORT TYPE AND DATES COVERED Final Subcontract Report, 1 July 1991 - 30 December 1993	
4. TITLE AND SUBTITLE Growth and Development of GaInAsP for Use in High-Efficiency Solar Cells		5. FUNDING NUMBERS C: XM-0-19142-3 TA: PV421101	
6. AUTHOR(S) P. R. Sharps		8. PERFORMING ORGANIZATION REPORT NUMBER	
7. PERFORMING ORGANIZATION NAME(S) AND ADDRESS(ES) Research Triangle Institute P.O. Box 12194 Research Triangle Park, NC 27709		10. SPONSORING/MONITORING AGENCY REPORT NUMBER TP-451-7166 DE95000210	
9. SPONSORING/MONITORING AGENCY NAME(S) AND ADDRESS(ES) National Renewable Energy Laboratory 1617 Cole Blvd. Golden, CO 80401-3393		11. SUPPLEMENTARY NOTES NREL Technical Monitor: J. Benner	
12a. DISTRIBUTION/AVAILABILITY STATEMENT		12b. DISTRIBUTION CODE UC-1264	
13. ABSTRACT (<i>Maximum 200 words</i>) This report describes accomplishments during Phase III of this subcontract. The overall goals of the subcontract were (1) to develop the necessary technology to grow high-efficiency GaInAsP layers that are lattice-matched to GaAs and Ge; (2) to demonstrate high-efficiency GaInAsP single-junction solar cells; and (3) to demonstrate GaInAsP/Ge cascade solar cells suitable for operation under concentrated (500X) sunlight. The major accomplishments during Phase III include (1) demonstrating a GaInAsP tunnel diode for use as an interconnect in the GaInAsP/Ge cascade cell, and (2) demonstrating a GaInAsP/Ge cascade cell. The development of the GaInAsP tunnel diode is a major accomplishment because it allows for the GaInAsP and Ge cells to be connected without optical losses for the bottom Ge cell, such as a Ge tunnel diode would cause. The GaInAsP/Ge cascade cell development is significant because of the demonstration of a cascade cell with a new materials system.			
14. SUBJECT TERMS high efficiency ; gallium indium arsenic phosphide ; photovoltaics ; solar cells		15. NUMBER OF PAGES 38	
17. SECURITY CLASSIFICATION OF REPORT Unclassified		16. PRICE CODE	
18. SECURITY CLASSIFICATION OF THIS PAGE Unclassified		20. LIMITATION OF ABSTRACT UL	
19. SECURITY CLASSIFICATION OF ABSTRACT Unclassified			